

Anti-bacterial activity and anti-cancer agent studies of *punica granatum* peel-doped silver/calcium oxide nanocomposites derived from camel bone

Raiedhah A. Alsaiari¹, Esraa M. Musa^{1,2*}, Fatima A. Al-Qadri,¹ Mervate M. Mohamed¹,
Moustafa A. Rizk^{1,3}

1. Department of Chemistry, College of science and art in Sharurah, Najran University, Najran P.O. Box 1988, Saudi Arabia.

2. Central Veterinary Research Institute (CVRI), P.O. Box 8067, Al Amarat, Khartoum, Sudan.

3. Department of Chemistry, Faculty of Science, Suez Canal University, Ismailia, Egypt.

*Email corresponding author: emmusa@nu.edu.sa

Abstract:

The main objective of this research is to synthesize active nanoparticles Ag/CaO (NPs) with a cost-effective, eco-friendly, quick, simple and sustainable process for turning leftover camel bone into a renewable resource for useful applications. The reduction factor has been prepared from a plant extract of *Punica granatum* peel and calcium oxide (CaO) which was made by calcination of dried camel bone at 800 °C and contains a high level of calcium (Ca) 31.3%, then mixed with Ag metal by using the sol-gel technique. A number of methods were used: XRD, BET, X-ray spectroscopy, UV, IR, and FESEM to investigate the optical, morphological, and structural characteristics of Ag/CaO NPs. The results showed that *Punica granatum* peel extract was a very affordable, non-toxic, and easily accessible capping agent. The MTT assay was also used to evaluate cytotoxicity in the bio-reducing synthesis process. Furthermore, the biological activity of the nanoparticles was evaluated against bacteria as well as fungal strains. Nanoparticles exhibited strong activity against *S. aureus* and *E.coli*, with an inhibition zone of 7.0 ± 0.2 - 8.0 ± 0.2 mm respectively, with moderate activity against *C. albicans* 5.0 ± 0.1 mm. Also the cytotoxic potential of synthesized nanoparticles against colon cancer and DU-145, PC-3 cell lines. It could be noticed that Cao/Ag nanoparticles had the highest anticancer action versus A549 with $IC_{50} = 124.16 \pm 1.93$ μ g/ml at concentration > 500 μ g/mL. The Ag/CaO

nanocomposite has shown efficacy as a catalyst in the reduction of dyes such as 2-Nitrophenol > 95%. It is hence efficient for environmental applications.

Keyword: *Punica granatum* peel, Ag/CaO NPs, camel bone, Anti-microbial activity, anti-cancer, 2-Nitrophenol.

Introduction:

Nanoparticles demonstrated antibacterial activities, they have been the subject of wide research. Although silver nanoparticles are known for their strong antibacterial activity, they are also known for their toxicity and cell oxidative damage [1]. Calcium oxide nanoparticles have drawn interest due to their decreased toxicity, high basicity, and histocompatibility [2] as well as their prospective uses as drug delivery agents, absorbents, catalysts, and antimicrobial agents [3]. Numerous studies have demonstrated that doping metallic oxides with various metal cations may improve their antibacterial qualities [4, 5]. Ag-doped CaO nanoparticles has antibacterial efficacy was assessed against *S. aureus* and *E. coli*, two harmful pathogens. Human fibroblast cells were subjected to cytotoxicity examination utilizing the dimethylthiazol and diphenyltetrazolium bromide [6]. It synthesizes nanocatalysts using non-noble metals like calcium (Ca) because it performs similarly to noble metals but at a significantly lower cost, noble metal-based catalysts are costly for real-world use. [7]. Significant worldwide worry is the emergence of bacterial resistance to traditional antibacterial medications as a result of their excessive and unnecessary use [8]. Water pollution is becoming a major issue due to the existence of several contaminants in water resources, such as organic dyes, nitroaromatic compounds, and microplastics [9]. Dyes and pigments are widely used for a variety of purposes. Almost all of the colors are harmful to aquatic life. Nevertheless, they are environmentally stable and scarcely biodegradable unless a catalyst is present [10]. *Punica granatum L.* belongs to the family *Punicaceae*, which consists of just two species and one genus. *Pomegranate* is used in medical fields for various purposes [11]. A blood tonic [12]. Heal aphthae, diarrhea, and ulcers [13]. The trunk bark contains 10–15% tannin, which plays important role in the production of leather [14]. Preparations made up of different sections of *P. granatum* have

been applied to cancer therapy [15]. The fruit extract shows antiviral activity [16]. Anti-microbial effect due to its anthiocyans [17].

Material and Methods

2. Materials:

2.1. Plant material:

The *punica granatum* peel was bought locally from a Sharourah market. It was made up of dried exudates stuck to the myrrh tree's bark. Shown in figure no (1).

2.2. Preparation of extract:

punica granatum peel was thoroughly cleaned with running tap water to get rid of any dust, and then it was cleaned with distilled water. The sample was then well dried at room temperature on filter paper before being aseptically pulverized using a sanitized pestle and mortar. 10 g of *Punica granatum* peel powder were shaken in 100 ml of distilled water for 4hrs to create a 10% (w/v) aqueous extract of *Punica granatum* peel [18]. The preparation was then centrifuged for 10 minutes at 8000 x g, and the supernatant was removed to create a crude extract brownish in color. Before use, test tubes were placed in a refrigerator at 4°C.



Figure (1): Pomegranate *Punica granatum* peel.

2.3. Chemical constituents of *Punica granatum* peel extracts.

2.3.1. Gas Chromatography, Mass Spectrometer (GC.MS)

Chemical constituents was determined using (Shimadzu, Japan TQ8040-2010) gas chromatograph, fitted with Flame ionization detector (FID). Separation of sample was achieved using C18 column, serial number (us6551263H), of 0.25um film thickness, 30 meter length, 0.25 mm inner diameter, injection temperature 250.00C°. This procedure is based on the precipitation of crude

powder or serum protein before analysis. The samples were diluted with equal volume of different solvents and then diluted 1:1 methanol (100%) [19].

2.4. Characterization and Preparation of Ag-doped CaO (NPs):

Ag-doped CaO nanoparticles were synthesized via a Sol-Gel procedure [20].

Calcium chloride dihydrate ($\text{CaO}/2\text{H}_2\text{O}$, 99 %), silver nitrate (AgNO_3 , 99.8–100.5 %), and sodium hydroxide (NaOH , 98 %) from (Sigma-Aldrich -Germany).

- Ag-doped CaO nanoparticles were prepared via a sol-gel method.
- 20 ml of deionized water were used to dissolve (1-x) mol $\text{CaO}/2\text{H}_2\text{O}$ and mol AgNO_3
- Solution containing 2 mol $\text{C}_6\text{H}_8\text{O}_7\text{H}_2\text{O}$ was added into the above solution under continuous stirring.
- Wet gel is formed when keeping mixture in a water bath at 80 °C, at 150 °C it turns to dry gel
- Ag-doped CaO nanoparticles were obtained by calcining dry gel at 500 C

The obtained samples were designated as pure CaO 0.1% Ag-doped CaO and 0.5% Ag-doped CaO respectively. They were analyzed by (XRD) (PANalytical Empyrean), X-ray photoelectron spectroscopic (XPS) (Thermo Scientific K-Alpha), (FTIR), UV, TEM and (FESEM) (JEOL JMS 70000F).

2.5. Preparation of CaO catalyst from camel bone.

The camel bone was dried at 120°C for 16 hours. Then were undergoing calcination in a muffle furnace for 3 hours at temperatures of 900°C [21].The figure used shown (Fig.2-a).

2.6. Synthesis of bare and extract doped Ag/CaO NPs

Aqueous extract comprising 35 mL of water as a soluble solution of $\text{CaO}/2\text{H}_2\text{O}$ and AgNO_3 (4.9 g & 0.25 g) was agitated for 5 minutes at 90 °C. Then *punica* peel extracts in varying amounts (5 mL & 10 mL) were added as drops to two distinct pure solutions. In the meantime, a 0.5 M NaOH solution was added to maintain a pH of ~12. For two hours, the colloidal solution was vigorously agitated at 90°C. As a result, the precipitate was cleaned and centrifuged for nine

minutes at 7100 rpm. Then calcined in an oven at a steady 90°C until the water had evaporated.[22-24].The figure used shown (Fig.2, b).

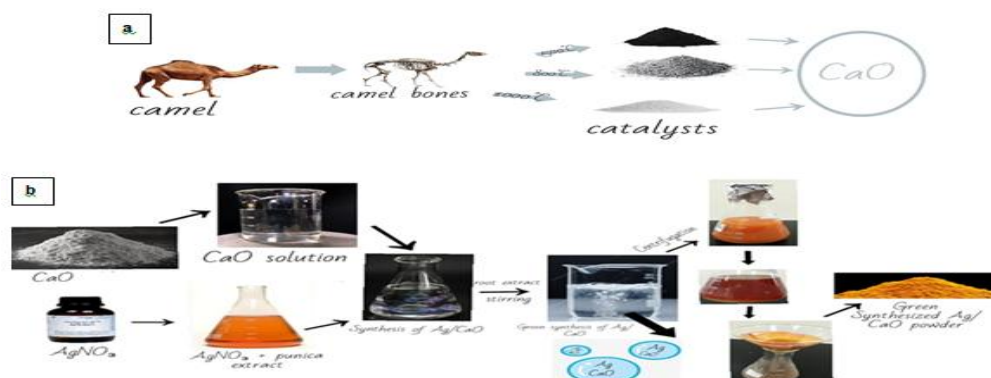


Figure (2- a, b): Diagram (a) preparation of CaO (b) extraction of *punica* peel synthesis of green synthesized Ag/CaO NPs.

2.7. Bacterial microorganisms:

2.7. 1. Isolation and identification of bacteria.

Pathogenic microorganisms (bacteria & fungi) were incubated on 5 % blood agar at 37 °C for 24–48 h [25]. Three isolated colonies from the standard colonies were obtained on Macconkey agars (MA) and mannitol salt (MS), respectively. Gram staining was developed by Burgey's Decisive Bacteriology Manual. Coagulase and catalase assays were used to confirm refined cell colonies morphologically and biochemically [26].

2.7.2. Antibacterial evaluation

The diffusion agar method was implemented to evaluate the materials under investigation *in vitro* antimicrobial features in opposition to a range of test pathogenic microorganisms, as shown in Table 1. The plates made from Mueller Hinton agar were used for bacteria, where is malt extract medium used for molds. The evaluated items were then placed onto the medium-made well using a scraped corn borer edge. Gentamicin (0.06 mg/ml) and fluconazole (0.28µg/ml) were often provided drugs, with DMSO acting as the baseline, the inhibiting radius was assessed at 38°C for bacterial cells, 4–8 days, and 27°C for the studied fungal species following a 72-hour growth period. Additionally, in compliance with the CLSI procedure, the micro-dilution process used to determine the minimum inhibitory concentration (MIC) of tested item [27].

Table (1): Reference of pathogenic microorganisms

<i>Bacillus subtilis</i>	NCTC 8236 (Gram + ve bacteria)
<i>Escherichia coli</i>	ATCC 25922(Gram -ve bacteria)
<i>Pseudomonas aeruginosa</i>	ATCC 27853 (Gram -ve bacteria)
<i>Staphylococcus aureus</i>	ATCC 25923(Gram +ve Bacteria)
<i>Candida albicans</i>	ATCC 25926 (Fungi)

National Collection of Type Culture (NCTC), Colindale, England.

American Type Culture Collection (ATCC) Rockville, Maryland, USA.

2.8. Evaluation of cytotoxicity against cancer colon DU-145 and PC-3 cell lines:

The experiment was done to assess the specimen's impact on the viability of the cell lines, MTT test was employed. Penicillin (110.0 units/mL), streptomycin (111 mg/mL), and heat-inactivated fetal bovine serum (14%) were incorporated to DMEM base, which was then moistened and kept at 36°C with CO₂ (9% v/v). After adding 120.0 µL of dispersed cell suspensions with 5.8×10^3 cells, 96-well plates were left to culture for an entire day. Following the addition of varying quantities of the specimens to the cell media, the developing cells were treated with 99.90 µL of the specimen-preserving media for three days. After application of sample treatment, the cells had been fixed using 145 µL of 12% TCA instead of bovine serum and left for 60 minutes at 6°C. The cells were washed six times with deionized water prior to the elimination of TCA solution. The cells were left in air for 15 minutes at 28°C in a dark condition after addition of 75 µL of 0.5% w/v MTT solution. The absorption was determined at 565 nm was recorded using a reader (Tecan 398, USA) [28].

2.9. Statistical analysis:

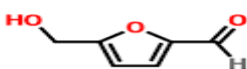
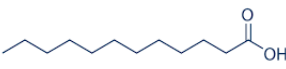
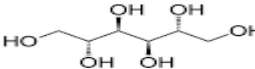
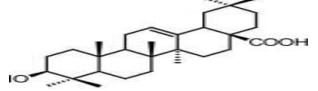
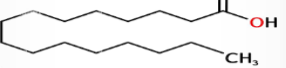

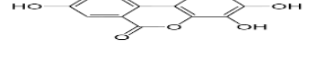
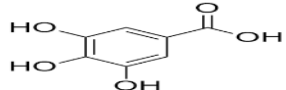
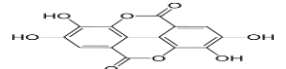
A statistical tool (SPSS 20) was utilized statistically to determine the antibacterial efficiency, which was presented by the diameter of the inhibitory zone (mm), using one-way analysis of variance (ANOVA). Analysis of molecular docking: Green-produced Ag/CaO nanoparticles were subjected to molecular docking studies in order to gain a better understanding of the mechanism behind their bactericidal effect [29].

3. Results and Discussion:

3.1. Chemical structures of *Punica granatum* peel extract:

Gas chromatography mass spectrometer (GC-MS) was used to determine the chemical structure of the peel of *Punica granatum*. The components were polyphenol and ellagic acid, 5-hydroxymethylfuraldehyde, lactic acid, palmitic acid, gallic acid, mannitol-manna sugar, oleanolic acid, and palmitic acid [30], as displayed in Table 2.

Table (2): Chemical structure detected by gas chromatography mass spectrometer (GC.MS) of aqueous extract of *Punica granatum* peel.

Name	Structure	Formula	Molecular weight
<i>Punica granatum</i>			
5-Hydroxymethylfuraldehyde		C ₆ H ₆ O ₃	126.11004 g/mol
Lauric Acid		C ₁₂ H ₂₄ O ₂	126.11004 g/mol
Mannitol-manna sugar		C ₆ H ₁₄ O ₆	182.17176 g/mol
Oleanolic acid		C ₃₀ H ₄₈ O ₃	456.71 g/mol
Palmitic acid		C ₁₆ H ₃₂ O ₂	256.4241 g/mol
Gallic acid		C ₆ H ₆ O ₃	170.11954 g/mol
Polyphenol		C ₆ H ₆ O	3500.2142 g/mol
Ellagitannin		C ₄₄ H ₃₂ O ₂₇	127.319 g/mol
Ellagic acid		C ₁₄ H ₆ O ₈	302.197 g/mol

3.2. Characterizations of calcined camel bone at 800°C

BET analysis as shown in Table 3. Catalyst calcined at 800 °C had a better crystalline order and higher surface area (15.7 m²/g), pore size (2.99 nm), and pore volume (0.023 cm³/g) [31]. By using TEM analysis of the hydroxyapatite

catalyst's particle size, the average size of the irregularly shaped grains ranges from 1.2 nm to 10 μm , as shown in Fig 3. These catalyst particles were not clearly shown to be hexagonal-shaped, similar to the XRD results, which is due to agglomerate formation on some particles [31].

Table (3): BET analysis of camel bone calcined catalyst at temperatures 800°C

No	Surface area (m^2/g)	Pore Size (nm)	Porevolume (cm^3/g)
800 °C	15.7	2.99	0.023

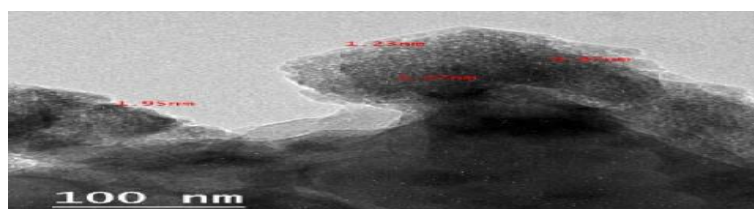


Figure 3. TEM image for calcined hydroxyapatite derived from waste camel bone.

3.2.1. XRD analysis.

Mineral salts (Na, Mg, P, K and CaO) have been measured in heat treated camel bone at 800°C. It was demonstrated that it had elevated calcium oxide levels 40.3% and moderate level of sodium 23.58%, magnesium 19.48%, potassium 14.03% and phosphor 10.23% respectively [31-32]. As shown by XRD figure (4). The newly formed catalyst derived from waste camel bone is considered to have promising characteristics, with an average particle diameter that allows for reuse in more than two cycles without losing activity.

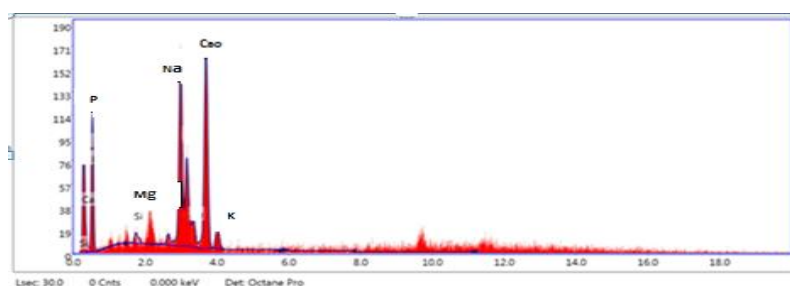


Figure (4): Measurement of mineral salts of camel bone treated at 800°C

3.3. Characterization of Ag-doped CaO nanoparticles:

3.3.1. Fourier- Transform Infrared Spectroscopy (FTIR)

The type of bonding found in the produced samples has been investigated using the FTIR [33]. Fig 5 shows the infrared spectrum of a silver-doped calcium oxide sample. The absorption band at 3743 cm^{-1} is likely due to the stretching of the O-H bond which may be present in the sample as a natural result of humidity [34]. Also, the absorption at 2321 cm^{-1} may be due to the bending of the C-H bond which may be due to the presence of traces of the plant extract residue [35]. The absorption peak at 954 cm^{-1} is due to the bending of the O-H bond [36]. The strong broad absorption peak at 1471 cm^{-1} and the strong sharp peak at 876.7 cm^{-1} indicate the formation of C-O bond due to the presence of carbonates resulting from the absorption of acidic carbon dioxide from the atmosphere by basic calcium oxide [37]. The sharp absorption peaks at wave numbers 1653 cm^{-1} and 2510 cm^{-1} are due to the stretching of the C-O bond [38]. The absorption spectrum at wavenumbers: 2982 cm^{-1} , 2874 cm^{-1} , 1636 cm^{-1} , 1387 cm^{-1} and 1072 cm^{-1} is a fingerprint for the presence of silver [39], especially the strong absorption at 668 cm^{-1} , which indicates the presence of Nano-sized silver particles[40]. There are no absorptions in the infrared region above the detection limit of the analysis, indicating the presence of the coesite mineral.

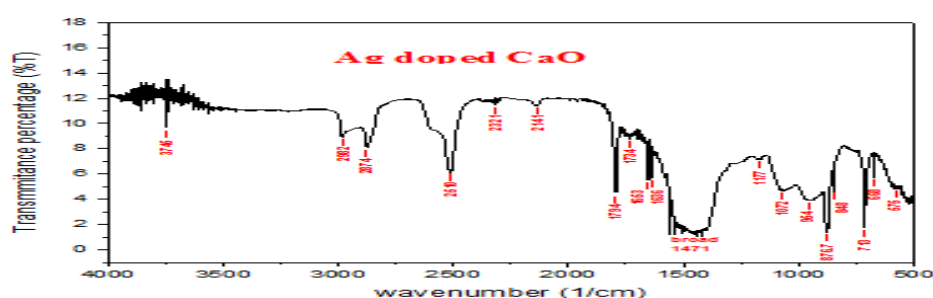


Figure (5): FTIR spectrum of Ag_xCa_{1-x}O nanoparticles

3.3.2. UV-Vis analysis spectra of the green synthesized

The UV-Vis analysis of Ag-doped CaO in figure 6 shows strong Surface Plasmon Resonance (SPR) centered at about 420-440 nm is characteristic of colloidal silver, which is triggered by the resonance of transmission band electrons

fluctuating together with the varying electric field of incident light to produce energetic plasmonic electrons during non-radioactive excitation [41].

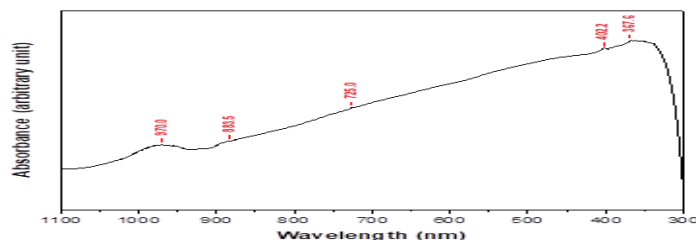


Figure (6): UV-Vis spectrum of Ag doped CaO nanoparticles

3.3.3. X-ray diffraction (XRD) analysis:

The X-ray powder diffraction analysis of Ag/CaO NPs composite [42]. Shows three crystalline minerals, the 1st of which was forms of silica (Coesite); the 2nd mineral was from calcium (Calcite). And the 3rd was silver it was observed that the sharp diffraction peaks corresponding to $2\theta=38^\circ$ and 44° were assigned to the directions from (111) and (200) planes corresponding to crystalline elemental silver (JCPDS 87-0717). The presence of these minerals was confirmed by EDX elemental analysis and the picture of Field Emission Scanning Electron Microscopy (FESEM) analysis, illustrated in figure (7).

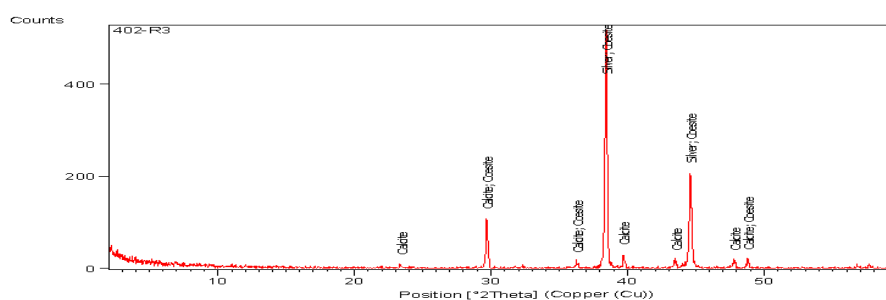
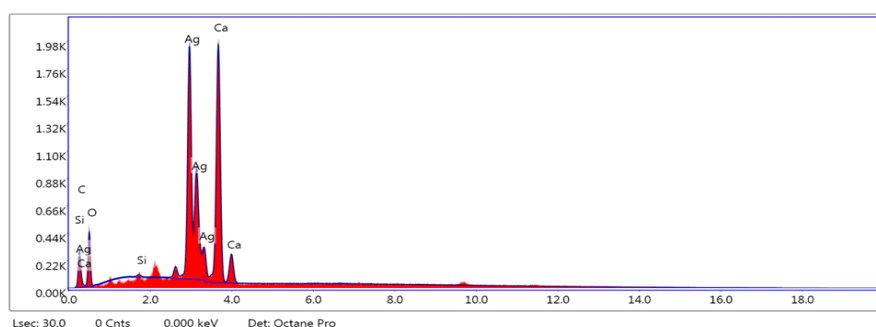


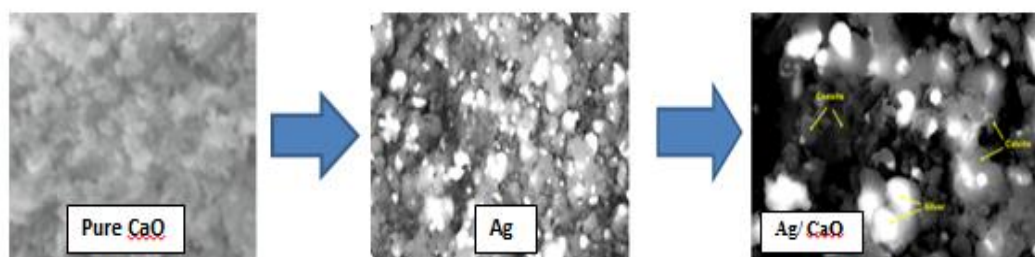
Table (4): Measurement of mineral salts of Ag doped CaO.

Element	Weight %	Atomic %	Net Int	Error	%
C	5.46	25.73	29.50	10.18	
Oxygen	26.30	58.35	52.33	12.72	
Si	0.08	0.41	5.38	51.98	
Ag	37.04	4.81	113.22	6.68	
Ca	42.3	10.70	127.84	5.25	

**Figure (8):** Measurement of mineral salts of treated of Ag doped CaO at 500°C

3.3.5. Field Emission Scanning Electron Microscopy (FESEM) analysis:

The image (9) shows calcium oxide (CaO) with irregular spherical shape, where silver (Ag) particle size increases as the percentage of Ag doping increases. Furthermore, Ag-doped CaO nanoparticles show aggregation of the three types of mineral grains. The silver grains are brightest with an average grain size of 12 nm, the calcite grains are medium bright with an average particle size of 12.5 nm, and the coesite grains are dark with an average grain size of 11 nm [44-45].

**Figure (9):** FESEM images of Ag doped CaO

3.4. Reduction of 2-Nitrophenol doped Ag/CaO NCs:

As shown in figure (10-a,b), evaluation of the effectiveness of Ag-doped CaO at various catalyst weights, such as 5 and 10 mg. Using a 2-NP solution prepared at a concentration of 0.25 mm, 2-nitrophenol (2-NP) using a reducing agent NaBH_4 , 2-NP was changed into 2-AP. The reaction was carried out at room temperature [41]. Without the catalyst, the BH_4 ions were unable to convert 2-NP to 2-AP [41]. As seen by the CaO reduction percentage of 75% at 25 minutes, the Ag reduction percentage of 80% at 23 minutes, and the solution's continued pale yellow color. In the meantime, the spectrophotometer was used to track the catalytic reduction of 2-NP with Ag-doped CaO. When NaBH_4 was added, the solution's color changed from pale yellow to yellow as a result of the 2-nitrophenolate ion being developed. The reduction efficiency of catalyst at different catalytic weights 5 and 10 ml, the conversion efficiency of Ag-doped CaO was 89% (20 min), 92% (15 min), 95% (10 Sec), respectively. This is due to Ag/CaO NPs having a larger surface area, a smaller in size and being well dispersed, and its synergistic effect is important throughout the reduction process.

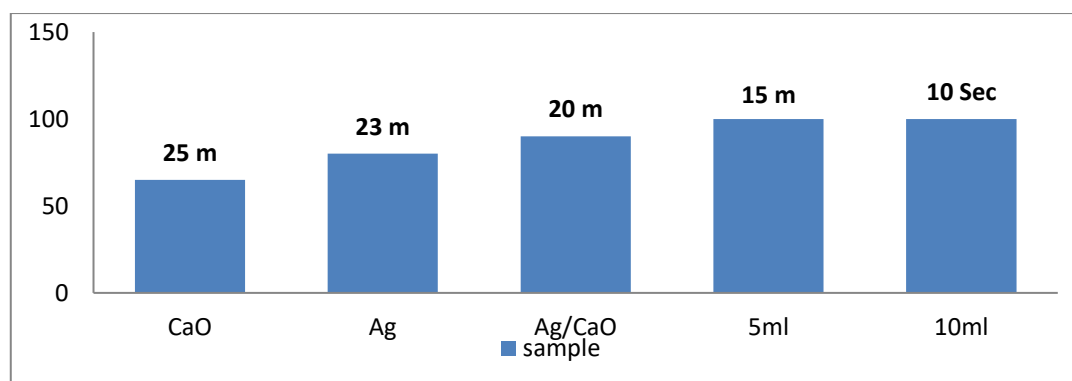


Figure (10-a): Catalytic reduction efficiency of 2-Nitrophenol using Ag doped CaO & time factor.

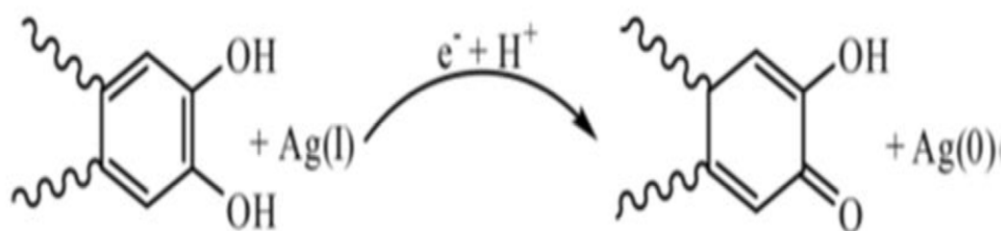


Figure (10-b): Biosynthesis mechanism of Ag NPs [41].

3.5. Antimicrobial activity of the tested Compounds

Evaluation of antimicrobial efficiency through monitoring microbial growth behavior in CFU/mL as a function of time allowed. Therefore, four distinct growth phases, lag, exponential growth, stationary growth, and death can be seen in the growth curves [46]. As showed in figure 11 & table 4, the anti-bacterial activity of silver-doped CaO nanoparticles is investigated against microorganism. The inhibition zone diameter for each disc is displayed. The material's toxicity increases with its concentration, against bacteria and a unicellular fungus strain. The studied compounds' capacity to suppress microbial growth was clearly evident. Furthermore, Ag/CaO nanoparticles exhibited the strongest activity against *S. aureus* and *E. coli*, with an inhibition zone of 7.0 ± 0.2 - 8.0 ± 0.2 mm respectively. Moderate against *C. albicans* 5.0 ± 0.1 mm compared to the standard drugs gentamicin and fluconazole 4.0 ± 0.3 & 3.0 ± 0.2 respectively. Moreover it could be noticed that, Cao/Ag (10 ml) had the highest action, while the impact had been reduced upon decreasing the concentration upon using Cao/Ag (5 ml). In accordance with other investigators who report that size and concentration of nanoparticles directly affect its activity [47-49]. The reason is presence of polyphenolic compounds and ellagitannin which are the main compounds of *Punica granatum* peel that form complexes with nanoparticles, they were chosen for molecular docking experiments in addition to Ag/CaO nanoparticles. This was achieved by concentrating on proteins that are necessary for the growth and

durability of bacteria. DNA gyrase, and dihydrofolate were among the numerous protein targets linked to distinct biosynthesis [50].

Table 4: Antimicrobial activity of the targeted extracts (Inhibition zone mm)

Sample code	Inhibition Zone (mm)				
	<i>P. aeruginosa</i>	<i>E. coli</i>	<i>B. subtilis</i>	<i>S. aureus</i>	<i>C. albicans</i>
CaO	1.0±0.3	2.0 ±0.1	3.0±0.2	7.0±0.2	3.0±0.2
Ag	2.0±0.4	3.0±0.2	3.0±0.2	3.0±0.2	3.0±0.4
CaO/Ag	3.0±0.2	4.0±0.1	3.0±0.2	5.0 ±0.2	4.0±0.1
5g	3.0±0.2	5.0±0.1	3.0±0.2	5.0 ±0.2	4.0±0.1
10g	4.0±0.2	8.0±0.1	4.0±0.2	7.0 ±0.2	5.0±0.1
Fluconazole ^a	-				3.0±0.2
Gentamicin ^b	3.0±0.3	5.0±0.3	3.0±0.1	5.0 ±0.2	-

Key: *M.D.I.Z : Mean diameter of growth inhibition zone in (mm).

** **Average of 2 replicates**; M.I.Z.D (mm): >18 mm: Sensitive (14–18)mm: Intermediate, < 14 mm: Resistant; (-)

***No inhibition zone.^a Fluconazole was used as standard antifungal and antibacterial agents at 25 µg/mL, respectively .

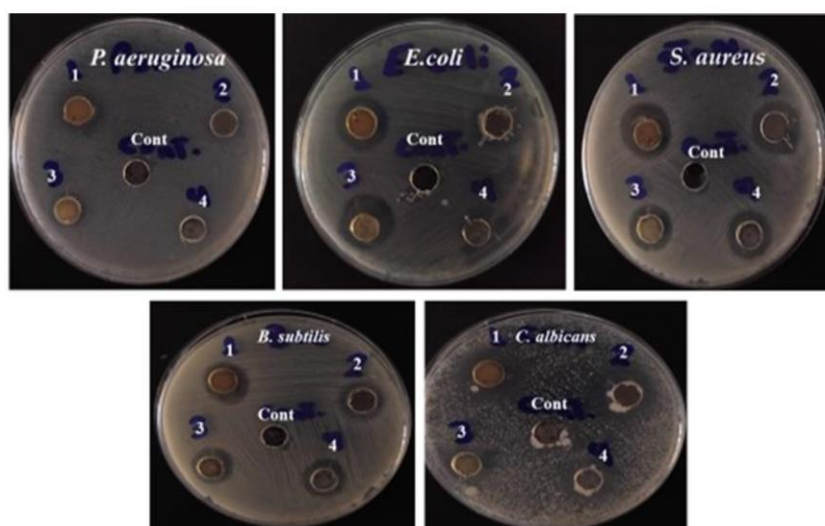


Figure (11): Antimicrobial impact of various examined specimens versus different bacteria and yeast strains.

3.6. Anti- microscopic observation of the cell lines treated with the Ag-doped CaO

As shown figures 12 & table 5, colony formation, migration, and proliferation were assessed. It was noticed that after 48 h the number of DU145 and PC3 cells was significantly ($p < 0.001$) reduced by Ag/CaO, which had been prepared using *Punica granatum* peel with the highest anti-cancer action versus A549 with an IC₅₀ of 124.16 ± 1.93 $\mu\text{g/ml}$ at concentration 500 $\mu\text{g/ml}$. In addition to silver (Ag), which had a moderate antitumor role versus A549 cells with an IC₅₀ of 264.16 ± 2.10 , CaO had a weak anticancer impact with an IC₅₀ of 314.10 ± 1.10 $\mu\text{g/ml}$, which decreased the number of colonies of both tested cell lines in the colony formation assay in comparison to the control (untreated group) in which cells appeared in the irregular shape, diffracted, multiple dents formed on the treated cell surface, cellular rounding up, shrinkage, and loss of cell adhesion [51]. The anti-cancer effect and toxicity of Ag/CaO nanoparticles via the colon cancer cell line increase with increasing concentration, as shown in figure (13).

Table 5. Anticancer impacts versus A543 cells of various levels (0-500 $\mu\text{g/ml}$)

Samples codes	Ag/Cao		Ag		CaO		Control	
Concentrations ($\mu\text{g/ml}$)	Viability %	Toxicity %	Viability %	Toxicity %	Viability %	Toxicity %	Viability %	Toxicity %
500	5.86	97.19	4.86	95.66	4.86	92.24	4.86	99.14
250	18.94	84.06	15.94	82.06	17.94	80.06	20.90	88.06
125	47.03	59.97	45.03	54.97	57.03	42.97	60.03	50.9
62.5	89.12	14.88	85.12	10.88	81.12	29.88	95.12	30.87
31.25	98.41	1.59	98.41	1.59	98.41	0.59	98.49	0.59
15.6	100	0	100	0	100	0	100	0
0	100	0	100	0	100	0	100	0
IC ₅₀ ($\mu\text{g/ml}$)	124.16 \pm 1.93		264.16 \pm 2.10		314.16 \pm 2.10		-	

of various treatments where outcomes are recorded as means \pm SD).

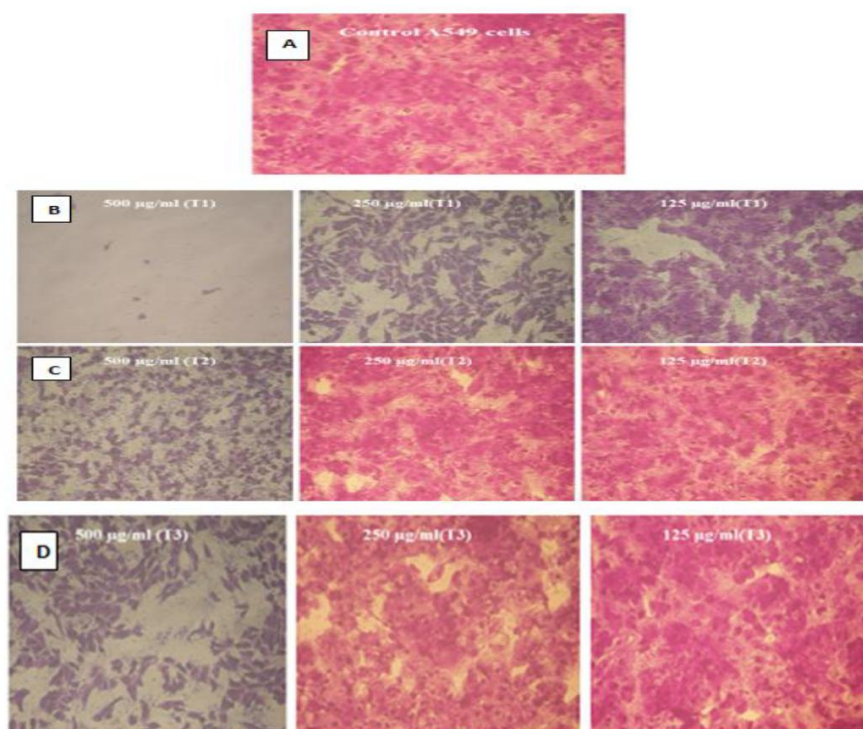


Figure (12): Microscopic observation of the cell lines treated with the compounds various: control (A); Ag/CaO (B); Ag (C); and CaO (D) via stereomicroscope (Magnification=400X).

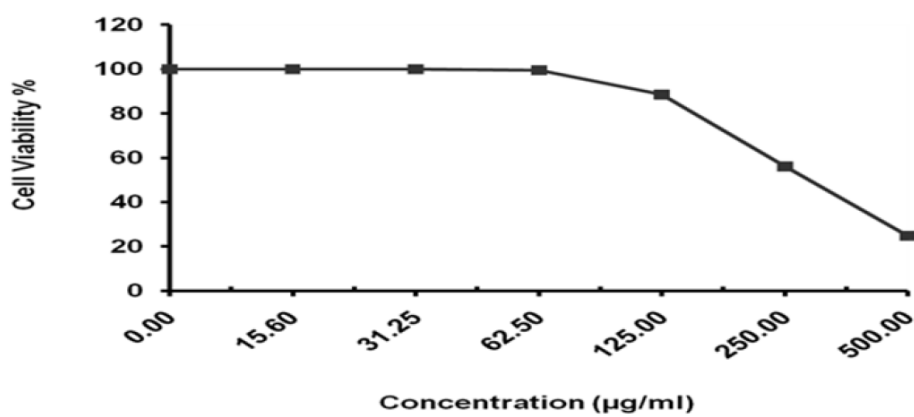


Figure (13): Relationship between concentration and cell toxicity (%).

Conclusion

The results prevailed that Ag/Cao NPs, which had been prepared by using *Punica granatum* peel, had a promising effect on the colon cancerous cell line and antimicrobial activity against bacteria and fungi. Also showed high conversion efficiency at 95% (10 sec). Recent investigations pointed out the successful roles of green synthesized nanoparticles to combat microbes used in a variety of ways to reduce infections and eradicate bacteria on food packaging, medical processes, and water treatment by damaging the membranes through their association or interacting with DNA and biomolecules, which leads to inhibition of cell multiplication and forming reactive oxygen species via their interacting with enzymes and/or biomolecules that cause cell damage or destruction. In addition, environmental research is influenced by the circular economy, which seeks to create sustainable resources from waste. For possible uses to lessen significant financial losses. Camel bone is sustainable resource for catalyst material that lessens the need for conventional chemical catalysts which may be eco-friendly.

Acknowledgment:

The authors are thankful to the Deanship of Graduate Studies and Scientific Research at Najran University for funding this work under Scholars Funding Program grant code (NU/FSP/SERC/13/254-2).

References

- [1] **Farid M Sroor, Ahmed F El-Sayed, Mohamed Abdelraof.** Design, synthesis, structure elucidation, antimicrobial, molecular docking, and SAR studies of novel urea derivatives bearing tricyclic aromatic hydrocarbon rings. *Archiv der Pharmazie*. (2024). e2300738
- [2] **Ahmed Sabt, Mohamad T Abdelrahman, Mohamed Abdelraof, Huda RM Rashdan.** Investigation of Novel Mucorales Fungal Inhibitors: Synthesis, In-Silico Study and Anti-Fungal Potency of Novel Class of Coumarin-6-Sulfonamides-Thiazole and Thiadiazole Hybrids. *ChemistrySelect*. (2022).7 (17): e202200691.

- [3] **Nakazato, G. Kobayashi, R.K.T, Seabra, A.B, Duran, N.** Use of nanoparticles as a potential antimicrobial for food packaging, *Food Preserv.*, Elsevier (2017) 413– 447. <https://doi.org/10.1016/b978-0-12-804303-5.00012-2>.
- [4] **Butt, A.R. Ejaz, S. Baron, J.C. Ikram, M. S. Ali, S.** Applications, CaO nanoparticles as a potencial drug delivery agent for biomedical applications, *Diget J. Nomaterials Biostructures*. 10 (2015) 799–809.
- [5] **Marquis, G. Ramasamy, B. Banwarilal, S. Munusamy, A.P.** Evaluation of antibacterial activity of plant mediated CaO nanoparticles using *C.issus quadrangularis* extract, *J. Photochem. Photobiol. B Biol.* 155 (2016) 28–33.
- [6] **Zhu, X. Wu, D. Wang, W. Tan, F. Wong, P.K. Wang, X. Qiu, X. Qiao, X.** Highly effective antibacterial activity and synergistic effect of Ag-MgO nanocomposite against *Escherichia coli*, *J. Alloys Compd.* 684 (2016) 282–290.
- [7] **Rao, Y. Wang, W. Tan, F. Cai, Y. Lu, J. Qiao, X.** Influence of different ions doping on the antibacterial properties of MgO nanopowders, *Appl. Surface Sci.* 284 (2013) 726–731.
- [8] **Y. Cai, Y. Wu, D. Zhu, X. Wang, W. Tan, F. Chen, J. Qiao, X. Qiu, X.** Sol-gel preparation of Ag-doped MgO nanoparticles with high efficiency for bacterial inactivation, *Ceramics Int.* 43 (2017) 1066–1072.
- [9] **Nivetha, I. Prabha, B.** Surfactant-enhanced nano spinel oxide for applications in catalysis, dye degradation and antibacterial activity, *Chemistry Select*, 7(33), (2022) e202202389. <https://doi.org/10.1002/slct.202202389>.
- [10] **Dai, R., Chen, J., Lin, J., et al.** Reduction of nitro phenols using nitroreductase from *E. coli* in the presence of NADH', *J. Hazard. Mater.*, 2009, 170, (1), pp. 141–143
- [11] **Aviram, M.; & Dornfeld, L.** Pomegranate juice consumption inhibits serum angiotensin converting enzyme activity and reduces systolic blood pressure. *Journal Atherosclerosis* (2001).158:195-198.
- [12] **Brochot A, Guilbot A, Haddioui L et al.** Antibacterial, antifungal, and antiviral effects of three essential oil blends. *Microbiology open* (2017) 6:e00459.
- [13] **Batta, A.K.; and Rangaswami, S.** Crystalline Chemical Components of Some Vegetable Drugs. *Journal Phytochemistry* .(1973), (12):214-216.
- [14] **Wynn, S.G.; and Fougere, B.J.** Introduction: why use herbal medicine. In: Wynn SG, Fougere BJ (ed) *Veterinary Herbal Medicine*. Library of Congress cataloging-in publication data. (2007). p 695,ISBN:10: 0-323-02998-1

- [15] **Shafaghat, A (Ph.D).** Phytochemical Investigation of Quranic Fruits and Plants. Journal of Medicinal Plants. Department of Chemistry, Islamic Azad University, Ardabil Branch, Ardabil, (2010). Iran.
- [16] **Schubert, S.Y. Lansky, E.P. Neeman, I.** Antioxidant and eicosanoid enzyme inhibition properties of pomegranate seed oil and fermented juice flavonoids. J. Ethnopharmacol. (1999). 66:11-17.
- [17] **Tanaka, T.; Nonaka, G.; Nishioka, I.** Tannins and Related Compounds. XLI. Isolation and Characterization of Novel Ellagitannins of *Punica granatum* L. J.Chem. Pharm. Bull. (1986). 34(2):656-63.
- [18] **Haider, A. Ijaz, M. Imran, M. Naz, M. Majeed, H. Khan, J.A. Ali, M.M. Ikram, M.** Enhanced bactericidal action and dye degradation of spicy roots' extract incorporated oxide nanoparticles (2019). Applied Nanoscience 10(2):3
[DOI: 10.1007/s13204-019-01188-x](https://doi.org/10.1007/s13204-019-01188-x)
- [19] **Hansen, L.** The Measurement of Serum and Urine Lithium by Atomic Absorption Spectrophotometry. Am. J. of Med. Tech. (1968).34, 1.
- [20] **Ramola, B. Joshi, N.C.** Green synthesis, characterizations and antimicrobial activities of CaO nanoparticles, Orient. J. Chem. 35 (2019) 1154–1157, <https://doi.org/10.13005/ojc/350333>.
- [21] **Woo, K.J. Hye, C.K. Ki, W.K. Shin, S. So, H.K. Yong, H.P.** Antibacterial activity and mechanism of action of the silver ion in *Staphylococcus aureus* and *Escherichia coli*, Appl. Environ. Microbiol. 74 (2008) 2171–2178, <https://doi.org/10.1128/AEM.02001-07>.
- [22] **Pal, S. Yoon, E.J Tak, Y.K. Choi, E.C. Song, J.M.** Synthesis of highly antibacterial nanocrystalline trivalent silver polydiguanylate, Chem. Soc. 131 (2009) 16147–16155, <https://doi.org/10.1021/ja9051125>.
- [23] **Huang, L. Yang, H. Zhang, Y. Xiao, W.** Study on synthesis and antibacterial properties of Ag NPs/GO nanocomposites, J. Nanomater 2016 (2016), <https://doi.org/10.1155/2016/5685967>.
- [24] **Jahan, I. Erci, F. Cakir-Koc, R. Isildak, I.** Microwave-irradiated green synthesis of metallic silver and copper nanoparticles using fresh ginger (*Zingiber officinale*) rhizome extract and evaluation of their antibacterial potentials and cytotoxicity, Inorg. Nano-Met. Chem. 51(2020) 722–732, <https://doi.org/10.1080/24701556.2020.1808017>.
- [25] **Abdul Salam, H. Sivaraj, R. Venckatesh, R.** Green synthesis and characterization of zinc oxide nanoparticles from *Ocimum basilicum* L. var.

- purpurascens Benth.-Lamiaceae leaf extract, Mater. Lett. 131 (2014) 16–18, <https://doi.org/10.1016/j.matlet.2014.05.033>.
- [26] **Haider, A. Ijaz, M. Imran, M. Naz, M. Majeed, J.A. Khan, M. Ikram, M.** Enhanced bactericidal action and dye degradation of spicy roots ' extract - incorporated fine - tuned metal oxide nanoparticles, A. Sci. 10 (2021) 1095–1104.
- [27] **Farid, M. Sroor, Ahmed, F. El-Sayed, Mohamed Abdelraof.** Design, synthesis, structure elucidation, antimicrobial, molecular docking, and SAR studies of novel urea derivatives bearing tricyclic aromatic hydrocarbon rings. Archiv der Pharmazie. (2024). 2024 Jun; 357(6):e2300738. Epub 2024 Mar 11. PMID: 38466125 [DOI: 10.1002/ardp.202300738](https://doi.org/10.1002/ardp.202300738)
- [28] **Al-Rajhi, A.M.H. Yahya, R. Abdelghany, T.M. Fareid, M.A. Mohamed, A.M. Amin, B.H. Masrahi, A.S.** Anticancer, Anticoagulant, Antioxidant and Antimicrobial Activities of *Thevetia peruviana* Latex with Molecular Docking of Antimicrobial and Anticancer Activities. Molecules. 2022 May 16;27(10):3165. [DOI: 10.3390/molecules27103165](https://doi.org/10.3390/molecules27103165).
- [29] **Snedecor, G.W. and Cochran, W.G.** Statistical Methods, 8th ed, Iowa State University Press, (1989). Iowa, USA.
- [30] **Fayez, M.B.E.; Negm, S.A.R.; Sharaf, A.** Constituents of Lokal Plants V. The Constituents of Various Parts of the Pomegranate Plant. J. Planta med. . (1963).11(4):439-43.
- [31] **Raiedhah, A. A. Esraa, M. M. Moustafa A. R.** Biodiesel production from date seed oil using hydroxyapatite-derived catalyst from waste camel bone' Heliyon 9 (2023) e15606. journal homepage: www.cell.com/heliyon.
- [32] **Haider, A. Ijaz, M. Ali, S. Haider, J. Imran, M. Majeed, H. Shahzadi, I. Ali, M.M. Khan, J. A. Ikram, M.** Green Synthesized Phytochemically (*Zingiber officinale* and *Allium sativum*) Reduced Nickel Oxide Nanoparticles Confirmed Bactericidal and Catalytic Potential, 50 (2020). Nanoscale Research Letters (2020) 15:50. <https://doi.org/10.1186/s11671-020-3283-5>.
- [33] **Nivetha a, A. Rakesh b, S.S. Priyatharshini, S.** Synthesis and structural characterization of Ag doped CaO for reduction of 2-Nitrophenol. Proc. Asian Res.Assoc, Vol1 : (2024) 115-119. [DOI: https://doi.org/10.54392/ara24112](https://doi.org/10.54392/ara24112)
- [34] **Chakma, S., J. B. Bhasarkar and V. S. Moholkar:** Preparation, characterization and application of sonochemically doped fe³⁺ into ZnO nanoparticles.IJRET.,02, 177-183(2013).

- [35] Ahmad, M., E. Ahmed, Z.L. Hong, N.R. Khalid, W. Ahmed and A. Elhissi: Graphene Ag/ZnO nanocomposites as high performance photocatalysts under visible light irradiation. *J. Alloys Compd.*, 577, 717–727(2013). <https://doi.org/10.1016/j.jallcom.2013.06.137>
- [36] Mallika, A.N., A. Ramachandra Reddy, K. Sowri Babu, Ch. Sujatha and K. Venugopal Reddy: Structural and photoluminescence properties of Mg substituted ZnO nanoparticles. *Opt. Mater.*, 36, 879–884(2014). <https://doi.org/10.1016/j.optmat.2013.12.015>
- [37] Wang, Y., J. Liu, L. Liu and D.D. Sun: Enhancing Stability and Photocatalytic Activity of ZnO Nanoparticles by Surface Modification of Graphene Oxide. *J. Nanosci. Nanotechnol.*, 12, 1–7(2012).
- [38] Shi, Q., J. Zhang, D. Zhang, C. Wang, B. Yang, B. Zhang and W. Wang: Red luminescent and structural properties of Mg doped ZnO phosphors prepared by sol-gel method. *Mater. Sci. Eng. B.*, 177, 689–693(2012).
- [39] Sankara Reddy, B. S. Venkatramana Reddy, N. Koteeswara Reddy and Pramoda Kumari, J. Synthesis, Structural, Optical Properties and Antibacterial activity of co - doped (Ag, Co) ZnO Nanoparticles. *Res. J. Material Sci* 1, 11–20(2013).
- [40] Chitra, K. and Annadurai, G. Antimicrobial activity of wet chemically engineered spherical shaped ZnO nanoparticles on food borne pathogen. *J. Food Research Journal* 20(1): 1829–1834 (2013) <http://www.ifrj.upm.edu.my>
- [41] Nivetha a, A. Rakesh b, S.S. Priyatharshini, S. Synthesis and structural characterization of Ag doped CaO for reduction of 2-Nitrophenol. *Proc. Asian Res. Assoc.* 1 (2024) 115–119 DOI: <https://doi.org/10.54392/ara24112>.
- [42] Volnianska, O. P. Boguslawski, J. Kaczkowski, P. Jakubas, A. Jezierski and E. Kaminska: Theory of doping properties of Ag acceptors in ZnO. *Phys. Rev. B.*, 80, 245212–1(2009). *Phys. Rev. B* 80, 245212 – Published 22 December, 2009. DOI: <https://doi.org/10.1103/PhysRevB.80.245212>.
- [43] Rajakumar, G. Thiruvengadam, M. Mydhili, G. Gomathi, T. Chung, I.M. Green approach for synthesis of zinc oxide nanoparticles from *Andrographis paniculata* leaf extract and evaluation of their antioxidant, anti-diabetic, and anti-inflammatory activities, *Bioprocess Biosyst. Eng.* 41 (2018) 21–30, <https://doi.org/10.1007/s00449-017-1840-9>.

- [44] Viswanatha, R., Y. ArthobaNayaka, C. C. Vidyasagar and T. G. Venkatesh. Structural and optical properties of Mg doped ZnO nanoparticles. J. chem. pharm. res., 4, 1983-1989(2012).
- [45] Iqbal, J., N. Safdar, T. Jan, M. Ismail, S.S. Hussain, A.Mahmood, S. Shahzad and Q. Mansoor. Facile Synthesis as well as Structural, Raman, Dielectric and Antibacterial Characteristics of Cu Doped ZnO Nanoparticles. J. Mater. Sci. Technol., 31, 300-304(2015). DOI: [10.1016/j.jmst.2014.06.013](https://doi.org/10.1016/j.jmst.2014.06.013)
- [46] Al-Rajhi, A.M.H, Mashraqi, A. Al Abboud, M.A. Shater, A.M. Al Jaouni, S.K. Selim, S. Abdelghany, T.M. Screening of Bioactive Compounds from Endophytic Marine-Derived Fungi in Saudi Arabia: Antimicrobial and Anticancer Potential. Life (Basel). 2022 Aug 3;12(8):1182. DOI: [10.3390/life12081182](https://doi.org/10.3390/life12081182).
- [47] Magdah A. Ganash, Abdel Ghany TM, Omar A.M. Morphological and biomolecules dynamics of Fusarium culmorum, and Alternaria alternata under stress of silver nanoparticles. Bio-NanoScience (2018). 8:566-573. <https://doi.org/10.1007/s12668-018-0510-y>.
- [48] Chandrakala, V. Aruna, V. Angajala, G. Review on metal nanoparticles as nanocarriers: Current challenges and perspectives in drug delivery systems. Emergent Materials (2022) 5:1593–1615 Emergent Materials. DOI: [10.1007/s42247-021-00335-x](https://doi.org/10.1007/s42247-021-00335-x)
- [49] Lai M-J, Huang Y-W, Chen H-C, Tsao L-I, Chang Chien C-F, Singh B, Liu BR. Effect of Size and Concentration of Copper Nanoparticles on the Antimicrobial Activity in *Escherichia coli* through Multiple Mechanisms. Nanomaterials. 2022; 12(21):3715. <https://doi.org/10.3390/nano12213715>.
- [50] Chidambara, M.K.N.; Jayaprakasha, G.K.; Singh, R.P. Studies on antioxidant activity of pomegranate (*Punica granatum*) peel extract using in vivo models. J. Agric. Food Chem. (2002). 50:4791-4795. DOI: [10.1021/jf010865b](https://doi.org/10.1021/jf010865b).
- [51] Alwhibi, M.S. Soliman, D.A. Khaldy, H.A. Alonaizan, A. Marraiki, N.A. El-Zaidy, M. AlSubeie, M.S. Green biosynthesis of silver nanoparticle using *Commiphora myrrh* extract and evaluation of their antimicrobial activity and colon cancer cells viability. Journal of King Saud University - Science, 2020; 32, (8): 3372-3379. <https://doi.org/10.1016/j.jksus.2020.09.024>.